Journal of Industrial and Engineering Chemistry xxx (2018) xxx–xxx

Contents lists available at ScienceDirect

Journal of Industrial and Engineering Chemistry

journal homepage: www.elsevier.com/locate/jiec

Improving understanding of solvent effects on intermolecular interactions in reactive liquid–liquid extraction with Isothermal Titration Calorimetry and molecular modeling

Lisette M.J. Sprakel, Boelo Schuur*

University of Twente, Faculty of Science and Technology, Sustainable Process Technology Group, The Netherlands

ARTICLE INFO

Article history:
Received 11 October 2018
Received in revised form 6 November 2018
Accepted 22 December 2018
Available online xxx

Keywords:
Liquid–liquid extraction
Crboxylic acids
Phenol
Isothermal titration calorimetry
Molecular modeling

ABSTRACT

Isothermal Titration Calorimetry (ITC) and molecular modeling (MM) were combined with liquid-liquid equilibrium data to obtain better understanding of solvent effects on complexation in reactive liquid–liquid extraction. Two examples with ample extraction literature available were studied, acetic acid extraction and phenol extraction. Interactions with binary solvents were studied. Based on the insight and quantification of complexation with MM and ITC, models describing the liquid-liquid equilibrium (LLE) were formulated and validated with experiments, showing that ITC can predict LLE. ITC together with MM indeed can yield additional insight in complexation behavior in reactive liquid–liquid extraction and may guide solvent selection procedures.

Introduction

Liquid–liquid extraction (LLX) is a commonly used technique with applications in the petrochemical industry [1], pharmaceutical industry [2–4], nylon industry [5], wastewater treatment [6] and fermentation processes [7–9]. For feed streams where one of the components is present in very low concentration, distillation is intrinsically inefficient [10]. Affinity based separation processes such as liquid–liquid extraction that address the dilute solute are promising alternatives for such dilute solute streams. With the changing orientation of the chemical industry towards more renewable feedstock, affinity separations become much more important [11]. Selection or design of the most appropriate solvent is not straight forward, as the solvent should preferentially have a high capacity and selectivity in the extraction step to reduce the solvent-to-feed ratio, but regeneration should also be possible to recycle the solvent and obtain the solute preferentially in concentrated streams. Good understanding of the intermolecular interactions in solvents that are typically reactive is required to find the best combination of good distribution in the primary separation, while allowing proper regeneration of the solvent.

For physical solvents a number of solvent screening approaches is available, e.g. based on linear solvation energy relationship (LSER) or the more expanded Abrahams model [12]. The drawback of these models is that new solvents first need to be parametrized based on distributions of solutes with known parameters, which is labor intensive. Alternatively, COSMO-RS may be applied [13], a software package deriving its parameters from quantum chemical calculations. This might still be time-consuming if the solvent is not in the database. For reactive solvents, affinity scales describing the interaction between extractants and solutes may be more applicable for solvent screening [14]. Examples of these scales are the BF_3-affinity scale for strong interactions and the pK_{BHX} hydrogen-bond basicity scale for weak interactions [15].

All of these approaches may yield initial screening results, after which in-depth studies are required, because typically conditions change between the extraction and regeneration and the effect of the conditions on the solvent is highly important information in the selection of a solvent and design of an LLX process [16]. Since this effect cannot be based on the affinity scales or empirical linear relationships, a good insight in and understanding of the mechanism and interactions of the complexation is required. We aim to obtain this insight by combining theoretical and practical methods, including direct homogeneous measurement of interaction energy through isothermal titration calorimetry (ITC), and molecular modeling (MM). The studies are complemented and

Abbreviations: HAc, acetic acid; IL, ionic liquid; IR, infrared; LLX, liquid–liquid extraction; MIBK, methyl isobutyl ketone; PhOH, phenol; TBP, tributylphosphate; TBPO, tributylphosphine oxide; TOA or Alamine 336, trioctylamine; TOPO, trioctylphosphine oxide.

* Corresponding author at: Drienerlolaan 5, Meander 221, 7522 NB Enschede, The Netherlands.
E-mail address: b.schuur@utwente.nl (B. Schuur).

https://doi.org/10.1016/j.jiec.2018.12.038
1226-086X/

Symbols

Symbol	explanation unit
A^-	Deprotonated anion of acid (–)
B	Base (–)
$c_{a,org}$,c_{org}	Concentration (of a) in solvent phase (M)
$c_{a,aq}$,c_{aq}	Concentration (of a) in raffinate phase (M)
c_0	Initial concentration (M)
ΔG	Gibbs energy change of a reaction (kJ/mol)
ΔH	Enthalpy change of a reaction (kJ/mol)
HA	Acid (–)
$[HA]$	Concentration of acid (M)
$[\overline{HA}\}$	Concentration of acid in organic phase (M)
$(HA)_nB_m$	(n,m)-acid–base complex (–)
H^+	Proton (–)
K_a	Acid-dissociation constant (–)
m	Number of bases in acid–base complex (–)
n	Number of acids in acid–base complex (–)
pK_a	Acidity (–)
pK_{BHX}	Hydrogen bond basicity (–)
K_c,K_E	Complexation constant ($M^{(n+m-1)}$)
$K_{D,a}$,K_D	Distribution coefficient of a (M/M),(–)
K_m	Physical extraction constant (–)
$K_{n,m}$	(n,m)-complexation constant ($M^{(n+m-1)}$)
ΔS	Entropy change of reaction (J/mol/K)
T	Temperature (°C)
Z	Extractant loading (–)

validated using liquid–liquid equilibria (LLE). With this approach, direct results are obtained on the complexation behavior between solvent and solute, and interpretation thereof is aided by MM. The extractions of acetic acid (HAc) and the less acidic phenol (PhOH) serve as case studies that were selected because of industrial relevance, resulting in ample literature being available, e.g. on extraction of acids from fermentation processes [7,8] and other biobased streams [17] and removal of phenol from wastewater [18,19], that can be used for comparison.

A key factor in extraction processes is the ratio of the distribution coefficient (Eq. (1)) in the forward extraction over the back-extraction [16]. The effect of operational parameters such as the choice of the diluent and the temperature on the intermolecular interactions between solute and extractant (and thus indirectly the distribution ratio) was studied with ITC and MM for extraction systems using tri-*n*-octylamine (TOA) [19–21], trioctylphosphine oxide (TOPO) and tributylphosphate (TBP) [22–27]. Extractant structures are given in Fig. 1. Based on the insights in the intermolecular interaction behavior with temperature and diluent composition, future research can be directed, not only with regard to solvent composition but also for extractant design. With the upcoming biorefinery separations, development of new LLX systems is highly important and may be aided using the combination of ITC and MM reported here.

Theory

The distribution ratio of an acid *HA* as defined in Eq. (1) results from a set of simultaneous equilibria displayed in Fig. 2. The overbar indicates organic phase compounds, and *B* is the extractant.

$$K_{D,a} = \frac{\overline{c_a}}{c_a} \tag{1}$$

Next to aqueous phase acid dissociation (K_a) and physical acid partitioning (K_m), complexes with B in various stoichiometries can be observed depending on the system and the conditions [28]. E.g. for tertiary amines, next to direct binding of the first acid to the amine, additional acid molecules can bind sequentially to the acid amine complex through hydrogen bonding [28,29]. It is assumed that the interactions of all sequentially hydrogen bonding acids are identical, but may be different from the interaction of the first acid with the amine. The example in Fig. 3a [28] shows proton transfer from the first acid to the extractant, whereas also extraction mechanisms in which hydrogen bonding is the dominating interaction for the first acid have been reported [22,28,30].

To account for the difference in interaction of the first acid and following acids with the extractant, a consecutive reactions model can be applied in the case of overloading of the amine [31]. The first reaction is described in Eq. (2).

$$HA + B \rightleftarrows HAB \tag{2}$$

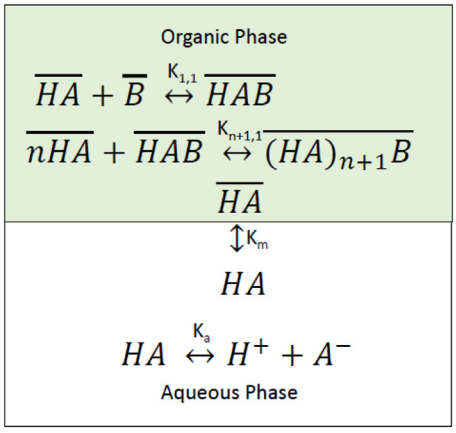

Fig. 2. Schematic overview of reactions in a liquid–liquid equilibrium.

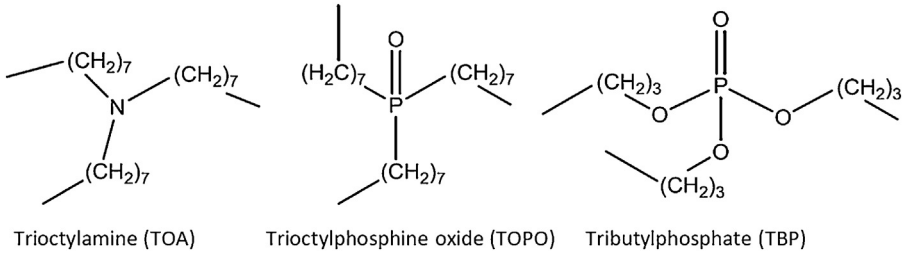

Fig. 1. Structure of extractants applied in this work.

Please cite this article in press as: L.M.J. Sprakel, B. Schuur, Improving understanding of solvent effects on intermolecular interactions in reactive liquid–liquid extraction with Isothermal Titration Calorimetry and molecular modeling, J. Ind. Eng. Chem. (2018), https://doi.org/10.1016/j.jiec.2018.12.038

In this reaction the (1,1)-complex is formed with reaction enthalpy $\Delta H_{1,1}$. The equilibrium constant of this reaction $K_{1,1}$ can be defined as:

$$K_{1,1} = \frac{[HAB]}{[HA][B]} \tag{3}$$

And the consecutive reactions are described in Eq. (4) as a lumped equation, which may be done assuming all hydrogen bond-based affinities are similar.

$$nHA + HAB \rightleftarrows (HA)_{n+1}B \tag{4}$$

In this reaction the (1,1)-complex reacts with n acid molecules to form the new complex, the reaction enthalpy of this reaction is $\Delta H_{n+1,1}$. The equilibrium constant of this reaction $K_{n+1,1}$ is defined as:

$$K_{n+1,1} = \frac{[(HA)_{n+1}B]}{[HAB][HA]^n} \tag{5}$$

Model extension for active diluent complexation

Active diluents such as 1-octanol may actively participate in complex formation [28,29,32,33]. For the active diluent 1-octanol (O), the reaction is described by Eq. (6), where *HAB* is the acid-extractant complex and *HABO* is the complex with the 1-octanol. Other active diluents such as chloroform interact similarly. Fig. 3b shows the complex formation between extractant TOA, acetic acid and the diluent.

$$O + HAB \rightleftarrows HABO \tag{6}$$

The equilibrium constant of this reaction $K_{1,1,O}$ is defined as:

$$K_{1,1,O} = \frac{[HABO]}{[HAB][O]} \tag{7}$$

ITC

With ITC any type of thermal interaction effects between molecules can be analyzed, and in a previous publication its applicability and accuracy for studying LLX was described [31]. From the titration curve the enthalpy of the reaction ΔH, the stoichiometry of complexation n and the binding association constant K, can be fitted to model equations. From these parameters ΔG and ΔS can be calculated, using Eqs. (8) and (9) [34]. By determining all thermodynamic parameters, ITC can provide insight in the extraction mechanism.

$$\Delta G = -RT\ln K \tag{8}$$

$$\Delta G = \Delta H - T\Delta S \tag{9}$$

Assuming a constant ΔH, the dependence of the equilibrium constant on temperature is given in Eq. (10), which is derived from Eqs. (8) and (9).

$$\ln\left(\frac{K_{T2}}{K_{T1}}\right) = -\frac{\Delta H}{R}\left(\frac{1}{T_2} - \frac{1}{T_1}\right) \tag{10}$$

The temperature dependent shift in equilibrium constant has a major effect on the shift in distribution ratio of the acid with a change of temperature.

The fitting parameters of the sequential binding model of Eqs. (2)–(5) are $K_{1,1}$, $K_{n+1,1}$, $\Delta H_{1,1}$, $\Delta H_{n+1,1}$ and n, and are fitted to the total energy released Q_{tot} in Eq. (11). For the model where the molecule of 1-octanol is incorporated in the complex, the total energy released is fitted to Eq. (12), including the additional fitting parameters $K_{1,1,O}$ and ΔH_3.

$$Q_{tot} = V_{tot}([HAB]\Delta H_{1,1} + [(HA)_{n+1}B](\Delta H_{1,1} + n\Delta H_{n+1,1}) \tag{11}$$

$$Q_{tot} = V_{tot}\Big([HAB]\Delta H_{1,1} + [(HA)_{n+1}B](\Delta H_{1,1} + n\Delta H_{n+1,1}) + [HABO](\Delta H_{1,1} + \Delta H_3)\Big) \tag{12}$$

Experimental

Chemicals

Chemicals were used without further purification and commercially obtained from Sigma Aldrich (acetic acid (HAc, >99.7%), phenol (PhOH, >99%), trioctylamine (TOA, 98%), trioctylphosphine oxide (TOPO, 99%), 1-octanol (>99%), heptane (99%), methylisobutylketon (MIBK, ≥99%), chloroform (≥99%), ethyl acetate (99.8%)), from Acros Organics (tributylphosphate (TBP, 99%)) and from VWR International (toluene (>99.5%)).

ITC

Isothermal Titration Calorimetry was performed on a TA Instruments TAM III Microcalorimeter, operated with the procedure

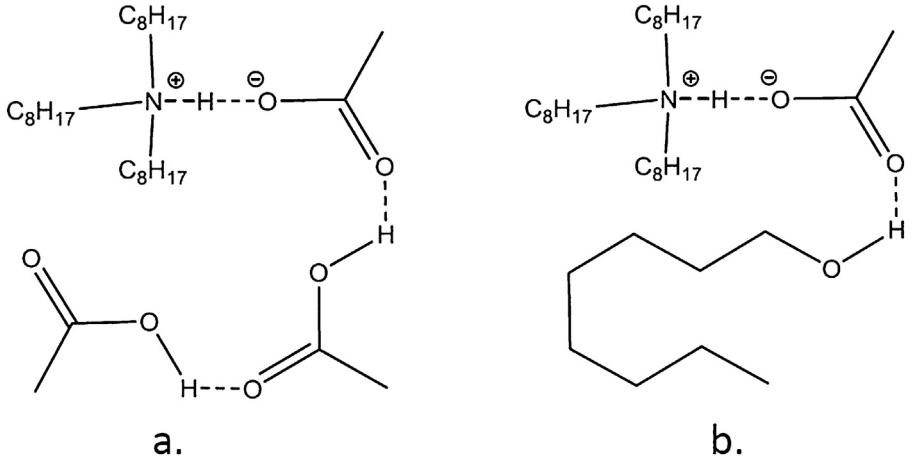

Fig. 3. Complex of trioctylamine with (a) three acetic acid molecules and (b) acetic acid and the active diluent 1-octanol.

Please cite this article in press as: L.M.J. Sprakel, B. Schuur, Improving understanding of solvent effects on intermolecular interactions in reactive liquid–liquid extraction with Isothermal Titration Calorimetry and molecular modeling, J. Ind. Eng. Chem. (2018), https://doi.org/10.1016/j.jiec.2018.12.038

previously described in [31]. For experiments with TBP a 1 mL sample vial was used that contained about 0.65 mL of organic solvent. Unless mentioned otherwise, the extractant concentration was 0.24 M. The injection volume was set between 5–20 μL and the injection interval was 75 min to ensure that the signal was back at the baseline level. In the case of acetic acid blank titration measurements were performed to correct for dilution of the titrant. For the experiment with 2.4 M TBP in heptane (>50 vol%) the data were corrected with the heat released from the last injection because the sample mixture is much more polar than the pure heptane in the blank measurement. For the experiments with phenol and TOA data were corrected with the energy released by the last injection because of the low *K*-value and heat release, whereas for TOPO and TBP the data were corrected based on the results of blank measurements. Previous work on a similar system of acetic acid and 0.24 M TOA with a parameter fit based on the sequential model of Eqs. (2)–(5) showed standard deviations of 11% in $K_{1,1}$, 4.2% in $\Delta H_{1,1}$, 26% in $K_{n+1,1}$, 12% in $\Delta H_{n+1,1}$ and 1.4% in n [31].

Liquid–liquid equilibria (LLE)

LLE experiments were performed by mixing 3 mL of aqueous acid solution with 3 mL of organic solution in 10 mL glass vials. The initial acetic acid concentration was 2.0 wt% and the initial phenol concentration was 1.0 wt%. Vials were extensively shaken by hand and vortex mixer, and then placed into a shaking water bath with a shaking speed of 200 rpm for 4 h. Thereafter the phases were allowed to settle for 1 h, after which samples were taken for analysis of the aqueous phase. Concentrations in the organic phase were determined by mass balance. The temperature in the shaking bath was set to either 20 °C or 60 °C.

HPLC

The aqueous phase of the LLE experiments was analyzed with an Agilent HPLC 1200 series equipped with a Refractive Index (RI) Detector (error ≤1%). The columns used are an Agilent Hi-plex H + Column (300 × 7.7 mm) or a GROM Resin H + IEX (250 × 8 mm) column, with a 5 mM H2SO4 solution mobile phase and a flow rate of 0.6 mL/min.

Molecular modeling

Molecular modeling of the intermolecular interactions was performed with Spartan'16 Parallel software from Wavefunction Inc. Interaction between two molecules can be described using the energy of the system of molecules as a function of the intermolecular distance. To obtain these profiles for the acids and extractants applied in this study, calculations were performed with a constrained distance between the acid and extractant modeled. For each distance, optimized geometries and energy profiles were calculated for the molecules with the Hartree–Fock 6-31G* level of calculation, since higher order calculations showed no significant improvement. Calculated energies were normalized by referencing them to systems with a very large intermolecular distance whose interaction energy was set at zero. For solvation the SM8 model was used in combination with the Hartree–Fock wavefunction, which is a parametrization for all atoms that treats the solvent as a continuous field. Reducing the carbon chain length of extractants with long hydrocarbon tails was applied to reduce the computation time. A comparison between complexes of trioctylamine (TOA) and tripropylamine (TPA) with up to 5 acid molecules showed that the structures and relative interaction energies of the complexes are not dependent on the carbon chain length of the amine. There is only an increase in the absolute interaction energy for the complex of the first acid with TOA, a direct result of the increased carbon chain length. This will however have a similar effect for all applied diluents and extractants.

Results and discussion

Typical ITC experiment

In Fig. 4 the results of a typical ITC experiment are displayed, in which acetic acid is titrated into the solvent comprising of 0.24 M TOA in toluene at 20 °C. In Fig. 4a the heat released by the reaction of the compounds is shown. The 'S-curve' in Fig. 4b is obtained by integrating the heat release from Fig. 4a. The first data point (at the lowest value of molar ratio) is very high. A deviant first data point is seen more often in the experiments and is probably caused by either air that is present in the injection line, diffusive loss of titrant [35] or an extra drop of titrant at the tip of the injection line. This integrated curve is used to fit the thermodynamic parameters of the system.

Fig. 5 shows the integrated ITC-results and sequential reaction model fit for an experiment in which the accuracy of the first part of the curve is improved by decreasing the injection volume of the first 4 injections. The larger negative $\Delta H_{1,1}$ (−23.2 kJ/mol) than ΔH_n

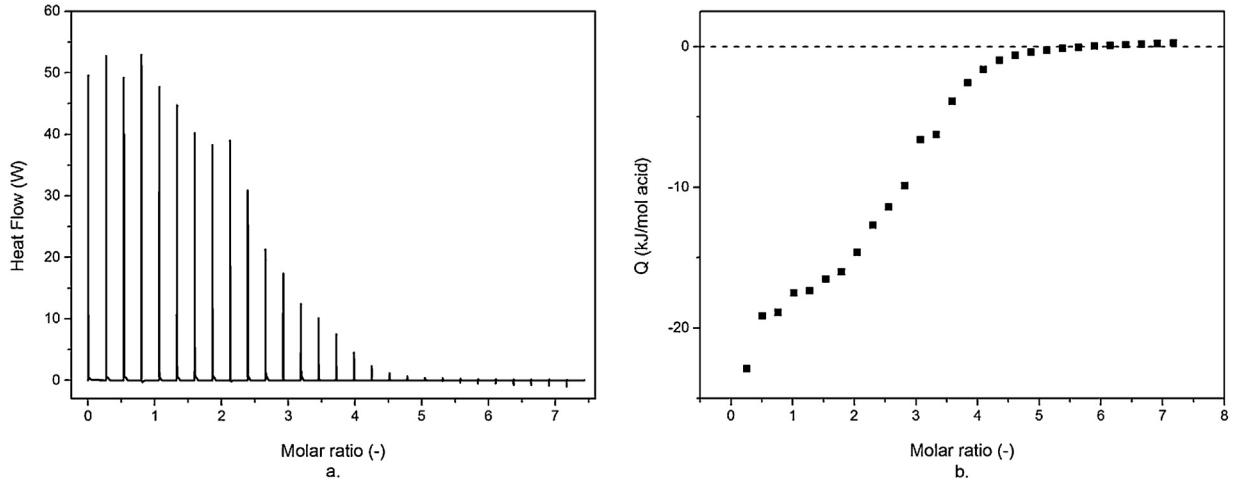

Fig. 4. ITC results for a typical experiment. (a) Heat flow of periodical titration of acetic acid to trioctylamine (0.24 M) in toluene at T = 20 °C, injection volume = 10 μL. (b) Integrated ITC curve.

Please cite this article in press as: L.M.J. Sprakel, B. Schuur, Improving understanding of solvent effects on intermolecular interactions in reactive liquid–liquid extraction with Isothermal Titration Calorimetry and molecular modeling, J. Ind. Eng. Chem. (2018), https://doi.org/10.1016/j.jiec.2018.12.038

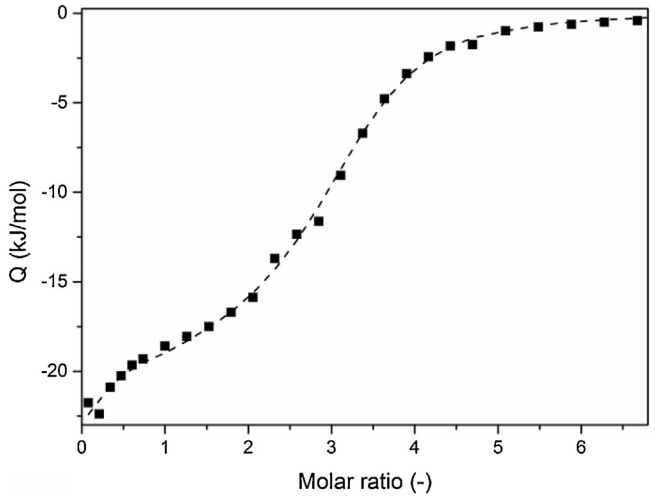

Fig. 5. ITC results for titrating acetic acid to trioctylamine (0.24 M) in toluene at T = 20 °C, injection volume = 3 μL, for first injection, 5 μL for injections 2–6, 10 μL for injection 7–21 and 15 μL for further injections. ■ experimental data, dashed line represents the sequential reaction model fit based on Eqs. (2)–(5).

$_{+1,1}$ (−20.0 kJ/mol) results from the double S-shape of the isotherm, and indicates that the first acid is bound stronger than the subsequent acids.

Solvent composition effects on complex formation

For each of the three extractants studied for acetic acid complexation, several diluents were applied. The results are displayed in Fig. 6, with 0.24 M TOA in Fig. 6a, with 0.24 M TOPO in Fig. 6b, and with TBP in Fig. 6c. In Fig. 6a, different types of curves can be distinguished. For TOA in chloroform, the heat effect is larger than for the other diluents and the first measurement point is very low compared to the rest, a typical problem with the first point that was also shown for the typical experiment in Fig. 4. TOA in 1-octanol results in the second largest heat effect, also reducing strongly around a molar ratio of 1. The other diluents all show the steep part at higher molar ratio. Where toluene and heptane exhibit a flat region in the beginning of the curve, MIBK and ethyl acetate show an increasing heat release.

The active and protic diluents chloroform and 1-octanol thus promote complexation indicated by the large heat release. Due to competitive hydrogen bonding of these diluents, a 1:1 stoichiometry is observed. The inactive diluents toluene and heptane exhibit lower energy release, but due to absence of hydrogen bonding with the diluent, multiple acids add to the complexes by hydrogen bonding. MIBK and ethyl acetate are active hydrogen bond accepting diluents, and the loss of hydrogen bonds between extractant and diluent results in a reduced net heat release at low stoichiometry. Their hydrogen bonds are less strong than the double hydrogen bonds between two acids, also resulting in overloading.

The effect of the diluent on the heat of complexation of acetic acid with TOPO (Fig. 6b), is different than for TOA (Fig. 6a). For the active and protic 1-octanol as a diluent the heat of complexation is almost negligible. The other diluents all show a steep decrease in heat of complexation around a stoichiometry of 1 acid per TOPO molecule, indicating 1:1 stoichiometry. Apparently the nature of the complexes does not favor additional interactions with acids. The inactive diluents toluene and heptane show a larger heat of complexation than the hydrogen bond accepting diluents MIBK and ethyl acetate. From this we can conclude that the interaction between TOPO and 1-octanol is of similar intensity as the interaction between TOPO and acetic acid. This effect might also be the reason why the heat of complexation is lower for MIBK and ethyl acetate.

Similar trends were obtained for the heat of complexation of acetic acid with TBP (Fig. 6c) although with a much higher TBP concentration because at 0.24 M it was not possible to obtain a proper 'S-curve'. It should be mentioned that from increasing the TBP concentration also a change in the *K*-value is expected, as *K* depends on extractant concentration [24,31,36]. For TBP no protic diluents were applied, since all other diluents showed already low heat of complexation and low complexation constants, visible through shallow slopes in the ITC-curves.

Fitting of the data

The isotherms in Fig. 6a were fit with the sequential binding model that allows the formation of two types of complexes, described by Eqs. (2) and (4). The fitted parameters are shown in Table 1 for complexation at a temperature of 20 °C.

Table 1
Fit parameters of ITC data on complexation of acetic acid with 0.24 M TOA in several diluents at T = 20 °C. Parameter fits are based on the sequential model in Eqs. (2) and (4).

Diluent	$\Delta H_{1,1}\left(\frac{kJ}{mol}\right)$	$K_{1,1}$	$\Delta H_{n+1,1}\left(\frac{kJ}{mol}\right)$	$K_{n+1,1}$	n
Toluene	−23.2	22.3	−20.0	68.5	1.6
Heptane	−17.9	22.5	−20.9	45.4	1.9
MIBK	−22.2	5.6	−20.4	47.5	1.5
Ethyl acetate	−24.6	5.9	−21.3	43.3	1.6
Chloroform	−50.0	15.0	−25.1	5.0	0.4
Water saturated 1-octanol	−38.0	97.1	−19.6	0.6	0.8
Unsaturated 1-octanol	−28.8	90.7	−27.6	0.8	0.8

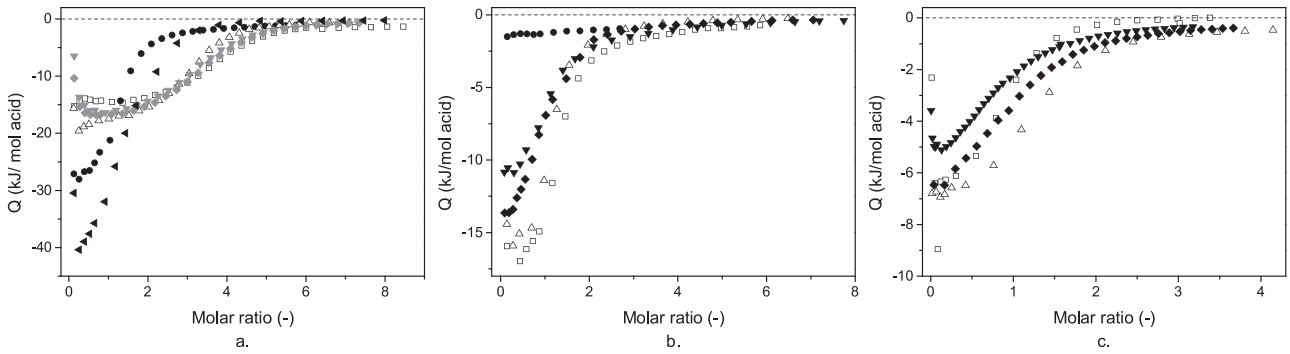

Fig. 6. Effect of diluent on ITC 'S-curve' for the net heat of complexation of the reaction of acetic acid and extractant in the active protic solvents ● 1-octanol, ◀ chloroform, in the hydrogen bond accepting solvents ◆ ethyl acetate and ▼ MIBK and in the inactive solvents △ toluene and □ heptane, with (a) 0.24 M TOA, (b) 0.24 M TOPO and (c) TBP (2.3 M in ethyl acetate, 1.1 M in MIBK, 1.8 M in toluene and 2.4 M in heptane).

Please cite this article in press as: L.M.J. Sprakel, B. Schuur, Improving understanding of solvent effects on intermolecular interactions in reactive liquid–liquid extraction with Isothermal Titration Calorimetry and molecular modeling, J. Ind. Eng. Chem. (2018), https://doi.org/10.1016/j.jiec.2018.12.038

From Table 1 it clearly reads that in the protic diluents 1-octanol and chloroform stronger 1:1 complexes are observed at higher $\Delta H_{1,1}$, whereas n and $K_{n+1,1}$ are lower than for non-protic diluents. When 1-octanol was saturated with water, the presence of water increased $\Delta H_{1,1}$ and $K_{1,1}$. For the hydrogen bond accepting diluents the typical signal showing initial increasing heat of complexation with increasing stoichiometry is indeed fitted with a higher $K_{n+1,1}$ than $K_{1,1}$.

The fit results for TOPO and TBP are given in Tables 2 and 3 respectively. The parameters were fitted using only the first reaction of the model, Eq. (2), since clearly no overloading occurs and applying extra equations decreases the accuracy of the parameter fit [31]. Fitting of the data for the diluents 1-octanol and chloroform appeared to be more difficult than for the other diluents, because there is no flat part in the beginning of the curve for the lower stoichiometry systems. Although the extractant concentration was taken into account for the fitting, comparing the results directly is difficult because of the influence of the concentration on $K_{1,1}$. No fit was possible at all for the energy of complexation with TOPO when 1-octanol was used, because the measured energy is too low.

Binary diluents

Mixtures of 1-octanol and toluene were applied in varying composition as binary diluents with extractant TOA to study the diluent composition effect on the complexation of TOA with acetic acid. The results are displayed in Fig. 7. For these experiments a high TOA concentration of 1 M was used to decrease the 1-octanol to TOA concentration ratio and to improve the slopes of the curves for easier comparison. It can be observed in Fig. 7 that with increasing 1-octanol fraction in the solvent the stoichiometry shifts down to favor more the (1,1)-complex being stabilized by 1-octanol.

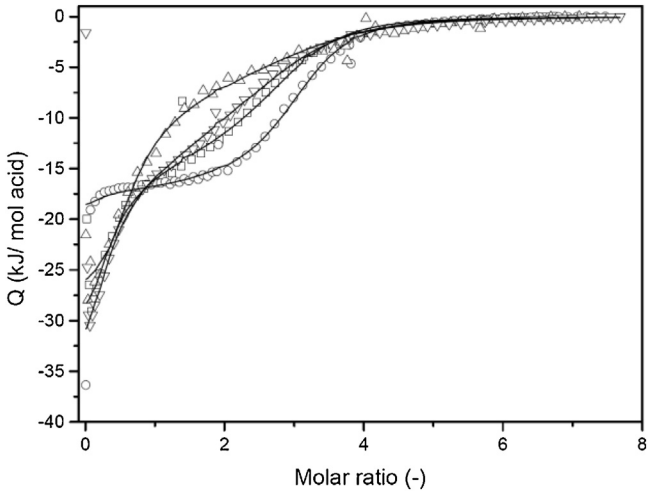

Fig. 7. Effect of 1-octanol concentration in the binary diluent of 1-octanol and toluene on the ITC 'S-curve' for the heat of complexation of the reaction of acetic acid with 1 M TOA (≈45 vol%) at 20 °C in: ○ 0% 1-octanol □ 50 vol% 1-octanol ▽ 75 vol% 1-octanol and △ 100 vol% octanol. Lines are fitted data with model parameters of Table 4.

Using Eqs. (2), (4) and (6), the ITC results of Fig. 7 were also fitted to determine the thermodynamic parameters. The results are shown in Table 4. Two trends are observed with increasing the volume fraction of 1-octanol, (1) a decrease of $\Delta H_{n+1,1}$ that is most likely a result of the competition between acetic acid and 1-octanol, and (2) a decrease of $K_{1,1}$, except for the 100% 1-octanol diluent, where also a decrease in all ΔH and K values is observed. In the solvent where the diluent only consists of 1-octanol, there is a 1-octanol to TOA ratio of 4. An explanation for the decrease in all parameters at this composition may be that this ratio of 1-octanol to TOA is too high for optimal complex solvation.

Effect of temperature

To study on the effect of temperature on acetic acid complexation with TOA in various diluents, ITC measurements were done at 60 °C and the thermodynamic parameters were fitted. These results are shown in Table 5. In general all K-values are lower than those at 20 °C (see Table 1). For the value of $K_{n+1,1}$ this effect is even stronger than for $K_{1,1}$. As a result, the average stoichiometry of the complexes is also lower at elevated temperature, which may be explained by reduced formation of hydrogen-bonds at elevated temperatures. In contrary to the observations for the other diluents, for 1-octanol that is not saturated with water, the value of $\Delta H_{1,1}$ significantly increases at increasing temperature, whereas $\Delta H_{n+1,1}$ reduces. This implies that in absence of water the interaction with the first acid is stronger at 60 °C than at 20 °C and the interaction of the following acids is weaker. This may also be explained by less favored

Table 2
Fit parameters of ITC data on complexation of acetic acid with 0.24 M TOPO in several diluents at T = 20 °C. Parameters are fitted based on the (1,1)-complexation in Eq. (2).

Diluent	$\Delta H_{1,1}$ (kJ/mol acid)	$K_{1,1}$
Toluene	−18	57
Heptane	−28	13
MIBK	−16	11
Ethyl acetate	−18	19
1-octanol	–	–

Table 3
Fit parameters of ITC data on complexation of acetic acid with TBP in several diluents at T = 20 °C. Concentration of TBP was 1.8 M in toluene, 2.4 M in heptane, 1.1 M in MIBK and 2.3 M in ethyl acetate. Parameters are fitted based on the (1,1)-complexation in Eq. (2).

Diluent	$\Delta H_{1,1}$ (kJ/mol acid)	$K_{1,1}$
Toluene	−7.9	2.9
Heptane	−22	0.3
MIBK	−6.2	3.7
Ethyl acetate	−9.1	1.2

Table 4
Fitted model parameters for complexation of acetic acid with 1 M TOA (≈45 vol%) in binary diluent of 1-octanol and toluene at 20 °C. Parameters are fitted based on the three complex model combining Eqs. (2), (4) and (6).

Vol% 1-octanol	$\Delta H_{1,1}\left(\frac{kJ}{mol}\right)$	$K_{1,1}$	$\Delta H_{1,1,o}\left(\frac{kJ}{mol}\right)$	$K_{1,1,o}$	$\Delta H_{n+1,1}\left(\frac{kJ}{mol}\right)$	$K_{n+1,1}$	n	$\frac{[O]}{[TOA]}$
0	−20.5	10.4	–	–	−18.0	19	1.7	0
50	−20.6	0.10	−11.2	48.5	−16.2	855	1.6	2
75	−24.0	0.030	−13.8	58.2	−15.3	622	1.4	3
100	−18.4	0.067	−10.4	30.6	−11.4	288	1.7	4

Please cite this article in press as: L.M.J. Sprakel, B. Schuur, Improving understanding of solvent effects on intermolecular interactions in reactive liquid–liquid extraction with Isothermal Titration Calorimetry and molecular modeling, J. Ind. Eng. Chem. (2018), https://doi.org/10.1016/j.jiec.2018.12.038

Table 5
Fit parameters of ITC data on complexation of acetic acid with 0.24 M TOA in several diluents at T = 60 °C. Parameters are fitted based on the sequential binding model in Eqs. (2) and (4).

Diluent	$\Delta H_{1,1}\left(\frac{kJ}{mol}\right)$	$K_{1,1}$	$\Delta H_{n+1,1}\left(\frac{kJ}{mol}\right)$	$K_{n+1,1}$	n
Toluene	−25.4	11.8	−23.7	10.5	1.4
Heptane	−18.5	13.4	−25.4	6.2	1.5
MIBK	−23.3	2.2	−18.9	19.5	1.5
Ethyl acetate	−26.2	2.8	−23.4	6.8	1.5
Unsaturated 1-octanol (0.36 M) TOA)	−39.2	12.5	−12.8	2.2	1.4
Water saturated 1-octanol	−38.6	14.0	−14.5	2.7	0.7

hydrogen-bonding at elevated temperatures. For the water-saturated 1-octanol there is no such effect since the presence of water can improve hydrogen bonding.

Extraction of phenol

The isotherms for the interaction of phenol with the three extractants measured with ITC are shown in Fig. 8, with the fitted parameters in Table 6. For each of the extractants in the complexation with phenol there is approximately a 1:1 ratio between phenol and extractant, therefore the data were fitted with the (1,1)-complexation reaction of Eq. (2). The release of energy from complexation with TOPO is larger than for the other two extractants. Compared with the data in Fig. 6, the *K*-values are clearly lower for complexation with phenol than for acetic acid in the case of TOA and TOPO. However, the *K*-values are difficult to compare since larger complexes ($n = 3$) are formed with TOA and the applied concentration of TBP is 0.36 M with phenol and 1.8 M with acetic acid.

The differences in affinity of acetic acid and phenol for the extractants are a result of the ability of the TOA to accept a proton from acetic acid, which is not possible for phenol [37]. Because the molecules of phenol cannot get ionized, TOA is not a suitable extractant for phenol. The weak interaction that is measured between TOA and PhOH further implies that also hydrogen bonding between TOA and PhOH is not strong enough to compete with the $\pi - \pi$ interactions between PhOH and the diluent toluene.

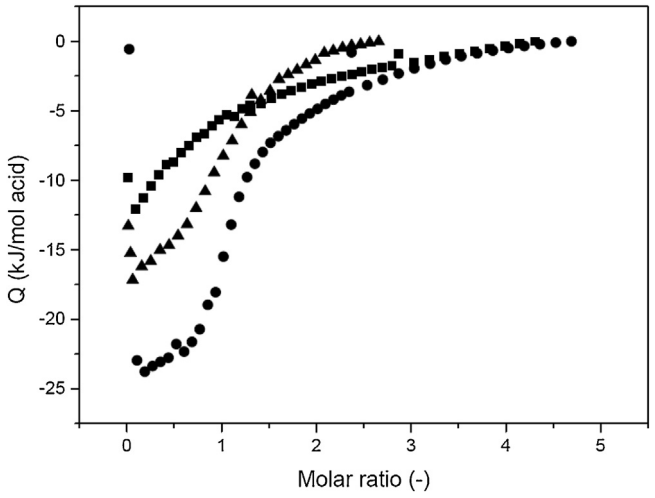

Fig. 8. Integrated ITC data for complexation with ■TOA (0.25 M), ● TOPO (0.21 M) and ▲TBP (0.36 M) in toluene for phenol at 20 °C.

Table 6
ITC results for complexation of phenol with TOA (0.25 M), TOPO (0.21 M) and TBP (0.36 M) in toluene at 20 °C, for ITC data of Fig. 8. Parameters are fitted based on the (1,1)-complexation in Eq. (2). Because of the low $K_{1,1}$ the error for the parameters for these results is up to a standard deviation of 20% in $\Delta H_{1,1}$ and 8% in $K_{1,1}$.

Extractant	$\Delta H_{1,1}$ (kJ/mol phenol)	$K_{1,1}$
gr	−20	5.7
TOPO	−55	8.7
TBP	−30	11

Validation of ITC data with LLE

To predict the distribution in biphasic extraction systems on the basis of ITC data, the acid dissociation constant of acetic acid ($=1.75 \times 10^{-5}$) [38] and the physical distribution of acetic acid are needed, as graphically illustrated in Fig. 2. The physical distribution was measured for the applied diluents, and the results are given in Table 7.

The calculated distribution coefficients using the complexation constants determined by ITC for acetic acid extraction with TOA in several diluents at 20 °C and 60 °C, or $K_{D,model}$, are compared with experimentally determined liquid–liquid equilibria $K_{D,LLE}$ in Fig. 9.

Table 7
Physical extraction of acetic acid by several diluents: distribution coefficients K_D of acetic acid (c_0 = 2wt%) in a liquid–liquid equilibrium with pure diluents at 20 °C and 60 °C.

Physical solvent	$K_{D,HAc}\left(\frac{M}{M}\right)$, T = 20 °C	$K_{D,HAc}\left(\frac{M}{M}\right)$, T = 60 °C
Heptane	0.00064 ± 0.020	0.0019 ± 0.020
Toluene	0.013 ± 0.020	0.015 ± 0.020
MIBK	0.48 ± 0.030	0.46 ± 0.030
1-octanol	0.46 ± 0.030	0.51 ± 0.031

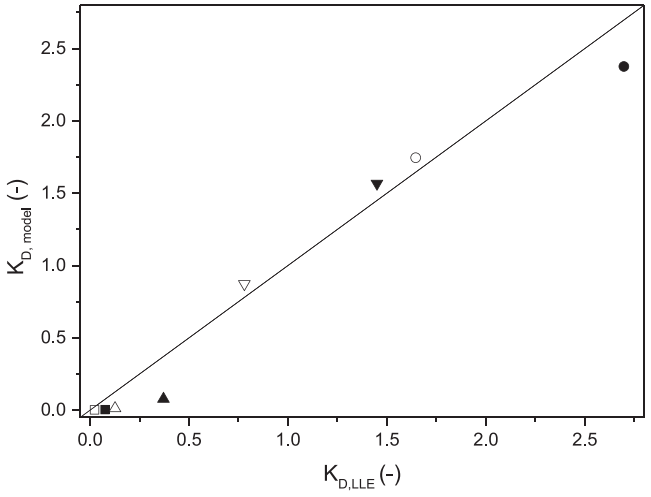

Fig. 9. Calculated distribution coefficients of acetic acid, or $K_{D,model}$, compared with experimentally determined values for liquid–liquid extraction of acetic acid (c_0 = 2 wt%) with 0.24 M TOA in several diluents: at T = 20 °C in ■ heptane, ▲ toluene, ▼ MIBK, and ● (water saturated) 1-octanol; and at T = 60 °C in □ heptane, △ toluene, ▽ MIBK, and ○ (water saturated) 1-octanol.

Please cite this article in press as: L.M.J. Sprakel, B. Schuur, Improving understanding of solvent effects on intermolecular interactions in reactive liquid–liquid extraction with Isothermal Titration Calorimetry and molecular modeling, J. Ind. Eng. Chem. (2018), https://doi.org/10.1016/j.jiec.2018.12.038

It follows that overall, the model based on ITC data successfully predicts the value of K_D for the diluents 1-octanol and MIBK reasonably well, although at lower values of $K_{D,LLE}$ there is underprediction, this might be an indication that dimerization in the organic phase should be taken into account to improve the model, since there is more dimerization in less polar diluents where also K_D is lower. However, incorporating dimerization as an extra equation in the fitting model for the ITC data also results in fitting of more variables, thereby reducing the accuracy of the fit.

Compared to acetic acid, phenol is a much weaker acid and also for this weaker acid the LLE was studied, and interactions with the extractants were studied in 1-octanol and toluene with ITC. For the experimental results in Table 8, the concentration of TOPO in the diluents is lower than for the other extractants due to limited solubility. From these results it is clear that higher values of K_D are obtained in the active diluent 1-octanol for the pure diluent and the TOA based solvent. For TOPO and TBP based solvents toluene shows higher values of K_D. Next to that, higher K_D is also obtained for phenol compared to acetic acid, which is due to the more hydrophobic nature of this molecule. In the diluent toluene π –π interactions between phenol and toluene contribute to the very high values of the distribution coefficient.

In contradiction to the case of acetic acid extraction, for extraction of phenols the tertiary amine TOA does not show the highest distribution, see Table 8. Similar results are reported in literature [39–42]. LLE experiments with TOPO, TBP and even pure 1-octanol result in a higher distribution coefficient than that in the case of TOA, although because of limited solubility the concentration of TOPO is only 11 wt% (≈0.24 M), compared to those of TOA (0.92M) and TBP (1.46 M).

Comparing the ITC and LLE results (Tables 1, 2, 3, 6 and 8) with the BF_3-affinity and pK_{BHX} scale [15], it can be concluded that for extraction of phenol the pK_{BHX} scale is more applicable since it clearly predicts high K_D for TOPO and TBP (taking into account the lower concentration of TOPO). For extraction of acetic acid with TOA in toluene the differences in K_D are too small to compare it with one of the scales, while for acetic acid in TOA in 1-octanol, where protonation of the extractant is expected, the BF_3-affinity scale clearly predicts the high K_D for TOA.

Molecular modeling

Aiming to understand the differences in mechanisms in the various systems, molecular modeling was used. For the interaction of both acetic acid and phenol with the three extractants TOA, TOPO and TBP energy profiles were created using a solvation model with 1-octanol and with toluene, see Fig. 10.

In the case of acetic acid interaction in 1-octanol (Fig. 10a), for all three extractants there is a (local) minimum visible at an intermolecular distance of 2 Å, characteristic for hydrogen bonding [43,44]. In addition, for TOA there is a minimum at a lower intermolecular distance around 1 Å, which is around the covalent bond distance for the N–H bond [38], which indicates a dative bond implying proton transfer. A deeper energy valley could be expected for proton transfer with TOA than for hydrogen bonding with TOPO and TBP, as proton transfer is a stronger interaction. It might be that neglecting interactions with surrounding water molecules influences the energy profile significantly. To study the influence of water molecules in the near vicinity of the complex, a simulation was run with five water molecules for a similar system comprising of trimethylamine and acetic acid, indeed confirming that in presence of water the characteristic proton transfer shows a deeper energy valley. In Fig. 10c, the results are shown for interaction between acetic acid and the extractants using toluene as a diluent. Here there is no (local) minimum at the typical distance of the N–H bond that would occur due to proton transfer, only at the distance for hydrogen bonding for all three extractants, so no proton transfer takes place between acetic and TOA when toluene is the diluent. The effect of diluent on the complexation of a tertiary amine and acetic acid was also studied with MM for the diluents chloroform, ethyl acetate, MIBK and heptane. Just as was the case for TOA in 1-octanol and toluene (Fig. 10a–c), for these diluents also two local minima are visible in the total energy. All diluents except 1-octanol show the lowest energy for hydrogen bonding, although for chloroform the local minimum around a proton transfer distance is relatively strong, followed by ethyl acetate and MIBK. Similar to toluene, for heptane the proton transfer state is even less favorable than the reference state in which there is no interaction.

With ITC (Table 1) it was also shown that for 1-octanol mainly the (1,1)-complex is formed and has a large enthalpy of complexation, followed by chloroform with a lower $K_{1,1}$ value. The difference between chloroform and the diluents MIBK and ethyl acetate is less clear in MM than in the ITC-data. It may be concluded that with the exception of chloroform, the findings of MM directly support the results from ITC (Table 1), where only for 1-octanol and chloroform larger differences between ΔH of the first and following acids were found, and only smaller differences in ΔH for the non-proton donating diluents as well as lower ΔH. No proton transfer was calculated for interaction between acetic acid and TOA in toluene, this is in accordance with the ITC results (Fig. 6a and Table 1) where TOA showed only a small difference in ΔH for the first and following acid interactions.

TOPO and TBP both only show an energy minimum at the typical distance of hydrogen bonding, with a larger energy value than TOA at that distance (Fig. 10a). This could not be compared with ITC results, since no isotherms could be measured for interaction of TOPO and TBP as a result of a too strong interaction between extractant and 1-octanol. The strong hydrogen bonding ability that is expected based on this interaction with 1-octanol is indeed visible in the MM results, also compared to TOA. In toluene (Fig. 10c), for TOPO and TBP also no proton transfer was calculated for interaction with acetic acid, which is in accordance with the ITC results (Fig. 6b and c and Tables 2 and 3).

The liquid–liquid equilibria in 1-octanol in Table 8 shows a very high K_D of acetic acid for TOA and a lower K_D for TBP and TOPO, which is in accordance with the proton-transfer that was only found for TOA using MM (Fig. 10a). The bond energy in molecular modeling is a bit higher for TOPO than for TBP in both 1-octanol and toluene (Fig. 10a–c). This can be related to the liquid–liquid equilibria, since the values for K_D are almost equal but TOPO was in LLE applied at a much lower concentration because of solubility limitations.

Fig. 10b shows the interaction between phenol and the three extractants TOA, TOPO and TBP in 1-octanol and Fig. 10d shows the

Table 8
Distribution coefficient K_D for phenol (c_0 = 1.0 wt%) and acetic acid (c_0 = 2.0 wt%) with different extractants at a temperature of 20 °C.

Solvent	$K_{D,HAc}\left(\frac{M}{M}\right)$	$K_{D,PhOH}\left(\frac{M}{M}\right)$	Solvent	$K_{D,HAc}\left(\frac{M}{M}\right)$	$K_{D,PhOH}\left(\frac{M}{M}\right)$
Pure toluene	0.013 ± 0.020	1.89 ± 0.058	Pure 1-octanol	0.46 ± 0.030	32 ± 4.0
TOA (40 vol% in toluene)	0.73 ± 0.012	10.3 ± 0.23	TOA (40 vol% in 1-octanol)	7.2 ± 0.17	30 ± 3.8
TOPO (11 wt% in toluene)	0.86 ± 0.038	185 ± 23	TOPO (11 wt% in 1-octanol)	0.75 ± 0.035	45 ± 5.6
TBP (40 vol% in toluene)	0.89 ± 0.038	210 ± 26	TBP (40 vol% in 1-octanol)	0.79 ± 0.036	117 ± 14

Please cite this article in press as: L.M.J. Sprakel, B. Schuur, Improving understanding of solvent effects on intermolecular interactions in reactive liquid–liquid extraction with Isothermal Titration Calorimetry and molecular modeling, J. Ind. Eng. Chem. (2018), https://doi.org/10.1016/j.jiec.2018.12.038

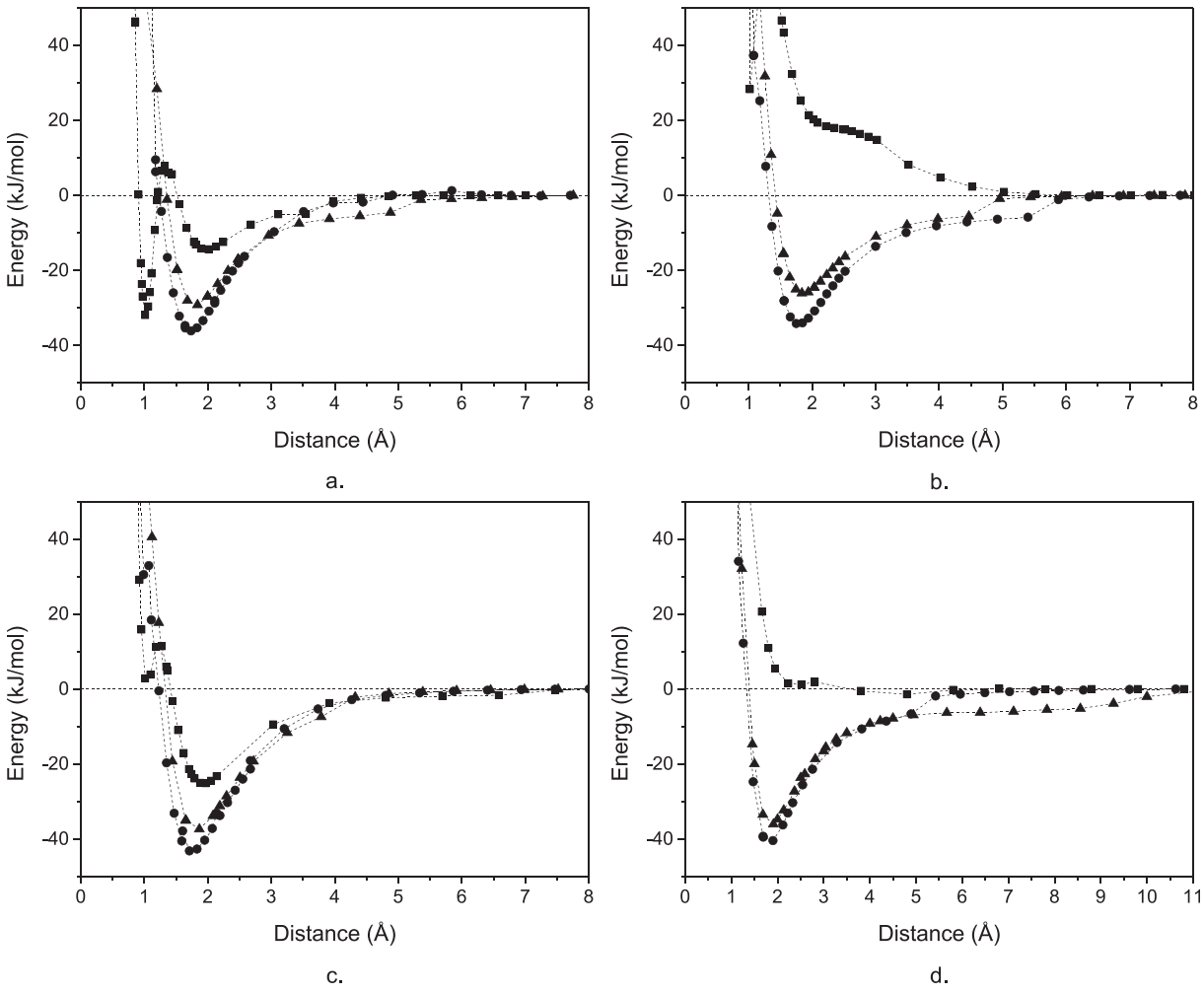

Fig. 10. Energy profile for varying the distance between the acid and extractant in complexation with ■TOA, ● TOPO and ▲TBP; calculated with Hartree–Fock 6-31G* wavefunction with SM8 solvation in 1-octanol, using Wavefunction's Spartan'16 Parallel, for (a) acetic acid in 1-octanol, (b) phenol in 1-octanol, (c) acetic acid in toluene and (d) phenol in toluene.

results in toluene. There is no energy minimum visible in the region of proton transfer in any of the graphs. For TOA there is also no energy minimum in the region of hydrogen bonding for both 1-octanol and toluene. Moreover, for both diluents the energy minimum is indicating a larger bond energy for TOPO than for TBP. Equal to the case of acetic acid, interactions of phenol with TOPO and TBP in 1-octanol could also not be analyzed with ITC, therefore only the modeling results for toluene can be compared with the ITC-results (Fig. 8 and Table 6). In these ITC measurements very little interaction with TOA was shown and TOPO showed more interaction, followed by TBP. This exactly matches the molecular modeling results and is also confirmed in the LLE results for the phenol-extractant system (Table 8), in which a very low K_D was found using TOA and high values of K_D were found for TBP and TOPO. Overall, it can be concluded that he use of MM strengthens the interpretation of the heat effects measured by ITC and together these two techniques can aid research on new solvents by allowing much better understanding of the intermolecular interactions that occur in solvent systems.

Conclusion

Isothermal Titration Calorimetry (ITC) was applied to directly characterize the thermodynamics of complexation in the study of liquid–liquid extraction of organic acids, and molecular modeling (MM) was used to aid interpretation of the ITC data. Complexation of acetic acid and phenol with extractants TOA, TOPO and TBP were studied in various diluents. It was found that the choice of diluent can affect the mechanism of the complexation, and that interaction between TOA and acetic acid has larger negative values of ΔH and larger complex stoichiometry than phenol. When protic diluents were applied the stoichiometry of the complexes was reduced because of competition between the acid and diluent, whereas inactive diluents resulted in more overloading of the amine. At elevated temperatures, all K-values are lower, where especially $K_{n+1,1}$ decreases strongly as a result of less tendency towards overloading of amine at elevated temperatures. In contradiction to the case of acetic acid, for phenol TOPO is a very suitable extractant, already at a concentration of only 11 wt% in 1-octanol TOPO outperforms the other extractants. The differences between interaction with phenol and acetic acid could be described using the BF_3-affinity scale for acetic acid and the hydrogen bond basicity pK_{BHX} scale for phenol, which was confirmed by ITC and MM.

The model based on ITC data can be used to predict LLE, and further interpretation by MM showed two local minima for the tertiary amine–acetic acid complex at typical distances for hydrogen bonding and proton transfer. For active diluents such as 1-octanol proton transfer is preferred and for the other diluents hydrogen bonding. This shows that the combination of ITC with MM is a strong approach to study the thermodynamics of

Please cite this article in press as: L.M.J. Sprakel, B. Schuur, Improving understanding of solvent effects on intermolecular interactions in reactive liquid–liquid extraction with Isothermal Titration Calorimetry and molecular modeling, J. Ind. Eng. Chem. (2018), https://doi.org/10.1016/j.jiec.2018.12.038

intermolecular interactions in liquid–liquid extraction processes and can help to improve the understanding of the interaction mechanism. Improved understanding of the effect of molecular structure of the extractant and diluent on the extraction and regeneration can help in the design of new solvents to improve solvent-based processes such as liquid–liquid extraction.

Acknowledgement

This is an ISPT (Institute for Sustainable Process Technology) project.

References

[1] R.A. Meyers, Handbook of Petroleum Refining Processes, 3rd edn., McGraw-Hill, New York, 2004.
[2] B.J.V. Verkuijl, B. Schuur, A.J. Minnaard, J.G. de Vries, B.L. Feringa, Org. Biomol. Chem. 8 (2010) 3045.
[3] B. Schuur, B.J.V. Verkuijl, A.J. Minnaard, J.G. de Vries, H.J. Heeres, B.L. Feringa, Org. Biomol. Chem. 9 (2011) 36.
[4] D. Rowley, H. Steiner, E. Zimmen, J. Soc. Chem. Ind. London 65 (1946) 237.
[5] M.L. van Delden, N.J.M. Kuipers, A.B. de Haan, Sep. Purif. Technol. 51 (2006) 219.
[6] P.R. Kiezyk, D. Mackay, Can. J. Chem. Eng. 49 (1971) 747.
[7] A. Krzyzaniak, M. Leeman, F. Vossebeld, T.J. Visser, B. Schuur, A.B. de Haan, Sep. Purif. Technol. 111 (2013) 82.
[8] Q.-Z. Li, X.-L. Jiang, X.-J. Feng, J.-M. Wang, C. Sun, H.-B. Zhang, M. Xian, H.-Z. Liu, J. Microbiol. Biotechnol. 26 (2016) 1.
[9] J. Hartl, R. Marr, Sep. Sci. Technol. 28 (1993) 805.
[10] M. Blahušiak, A.A. Kiss, S.R.A. Kersten, B. Schuur, Energy 116 (2016) 20.
[11] A.A. Kiss, J.-P. Lange, B. Schuur, D.W.F. Brilman, A.G.J. van der Ham, S.R.A. Kersten, Biomass Bioenergy 95 (2016) 296.
[12] J.-C. Bradley, M.H. Abraham, W.E. Acree, A.S. Lang, Chem. Cent. J 9 (2015) 12.
[13] F. Eckert, A. Klamt, AIChE J. 48 (2002) 369.
[14] M.T.G. Jongmans, A. Londoño, S.B. Mamilla, H.J. Pragt, K.T.J. Aaldering, G. Bargeman, M.R. Nieuwhof, A. t. Kate, P. Verwer, A.A. Kiss, C.J.G. van Strien, B. Schuur, A.B. de Haan, Sep. Purif. Technol. 98 (2012) 206.
[15] C. Laurence, J.-F. Gal, Lewis Basicity and Affinity Scales, John Wiley & Sons, Ltd., 2009.
[16] L.M.J. Sprakel, B. Schuur, Sep. Purif. Technol. 211 (2019) 935.
[17] B. Girisuta, L.P.B.M. Janssen, H.J. Heeres, Ind. Eng. Chem. Res. 46 (2007) 1696.
[18] B. Cuypers, A.T.M. Burghoff, E.J.R. Sudhölter, A.B. de Haan, H. Zuilhof, J. Phys. Chem. A 112 (2008) 11714.
[19] H. Uslu, D. Datta, H.S. Bamufleh, J. Mol. Liq. 212 (2015) 430.
[20] M.E. Marti, Sep. Sci. Technol. (2016) 1.
[21] C.B. Rasrendra, B. Girisuta, H.H. van de Bovenkamp, J.G.M. Winkelman, E.J. Leijenhorst, R.H. Venderbosch, M. Windt, D. Meier, H.J. Heeres, Chem. Eng. J. 176–177 (2011) 244.
[22] T. Hano, M. Matsumoto, T. Ohtake, K. Sasaki, F. Hori, Y. Kawano, J. Chem. Eng. Jpn. 23 (1990) 734.
[23] W. Cai, S. Zhu, X. Piao, J. Chem. Eng. Data 46 (2001) 1472.
[24] K.L. Wasewar, D.Z. Shende, J. Chem. Eng. Data 56 (2011) 288.
[25] T. Brouwer, M. Blahusiak, K. Babic, B. Schuur, Sep. Purif. Technol. 185 (2017) 186.
[26] M. Wisniewski, M. Pierzchalska, J. Chem. Technol. Biotechnol. 80 (2005) 1425.
[27] Y.Z. Yang, Y.H. Yang, G.X. Sun, X.J. Meng, Z.Q. Wang, S.X. Sun, Chem. J. Chin. Univ. 17 (1996) 515.
[28] J.A. Tamada, C.J. King, Ind. Eng. Chem. Res. 29 (1990) 1327.
[29] G.M. Barrow, E.A. Yerger, J. Am. Chem. Soc. 76 (1954) 5211.
[30] N. Masaru, S. Tatsuya, Bull. Chem. Soc. Jpn. 51 (1978) 705.
[31] L.M.J. Sprakel, B. Schuur, Ind. Eng. Chem. Res. (2018) 12574.
[32] K. Wang, Z. Chang, Y. Ma, C. Lei, S. Jin, Y. Wu, I. Mahmood, C. Hua, H. Liu, Fluid Phase Equilib. 278 (2009) 103.
[33] Y.K. Hong, W.H. Hong, Bioprocess. Eng. 22 (2000) 281.
[34] R.J. Falconer, A. Penkova, I. Jelesarov, B.M. Collins, J. Mol. Recognit. 23 (2010) 395.
[35] S.E. Boyce, J. Tellinghuisen, J.D. Chodera, bioRxiv (2015) 23796/23791-23796/23797.
[36] W. Qin, Z. Li, Y. Dai, Ind. Eng. Chem. Res. 42 (2003) 6196.
[37] S. Aono, S. Kato, J. Comput. Chem. 31 (2010) 2924.
[38] D.R. Lide, CRC Handbook of Chemistry and Physics, 74th edn., CRC Press, Boca Raton, 1993.
[39] C. Zidi, R. Tayeb, M. Dhahbi, J. Hazard. Mater. 194 (2011) 62.
[40] C. Zidi, R. Tayeb, M.B.S. Ali, M. Dhahbi, J. Membr. Sci. 360 (2010) 334.
[41] W. Cichy, Š. Schlosser, J. Szymanowski, J. Chem, Technol. Biotechnol. 80 (2005) 189.
[42] R. Gutierrez, A. Urtiaga, I. Ortiz, J. Chem. Technol. Biotechnol. 85 (2010) 1215.
[43] P. Gilli, L. Pretto, V. Bertolasi, G. Gilli, Acc. Chem. Res. 42 (2009) 33.
[44] L.I. Krishtalik, BBA-Bioenergetics 1458 (2000) 6.

Please cite this article in press as: L.M.J. Sprakel, B. Schuur, Improving understanding of solvent effects on intermolecular interactions in reactive liquid–liquid extraction with Isothermal Titration Calorimetry and molecular modeling, J. Ind. Eng. Chem. (2018), https://doi.org/10.1016/j.jiec.2018.12.038